Experimental Pressure Response for a Modified PRC: Well-Stirred Binary Gas Phase

S. M. S. Soares and R. G. Rice
Dept. of Chemical Engineering, Louisiana State University, Baton Rouge, LA 70803

The batch pressure-response cell provides flexible and accurate means of assessing the kinetics in heterogeneous gas-liquid reactions. A new model is derived to determine the kinetics of reactions of general (n,m) order using binary gas phase. This model has an important feature that allows the determination of the reaction order with respect to the gas-phase reactant and the rate constant from a single set of pressure vs. time data through a simple two-parameter estimation routine. Gas mixing was introduced via a simple modification of the liquid-phase magnetic stirrer to reduce the gas-phase mass-transfer resistance to negligible levels and the parameter estimation problem to only two factors. The heterogeneous cobalt catalyzed sulfite oxidation reaction at low partial pressures of oxygen using a nitrogen-oxygen mixture was tested to verify the validity of the model. The predicted kinetics were remarkably close to those values in the literature, yielding an oxygen order of 1.98 ± 0.02, which is taken to be second order in oxygen.

Introduction

In recent years, the batch pressure-response cell (PRC) has been used to assess the kinetics of heterogeneous gas-liquid reactions. The method has proven itself very flexible and capable of determining the kinetics of both linear (Rice and Benoit, 1986) and nonlinear (Bhargava, 1988; Rice et al., 1994) reactions. More recently, attempts were made to determine the kinetics of gas-liquid systems using a binary gas phase (nitrogen was used as inert diluent gas) (Rice et al., 1994). However, the apparatus they used did not have any means for stirring the gas phase (the only agitation being provided by the movement of the well-stirred liquid phase underneath the gas), and therefore the gas-side mass-transfer coefficient was small and variable. This somewhat stagnant gas phase brought up a problem of precision: the estimated mass-transfer coefficient had a somewhat important effect on the overall parameter estimation problem. Furthermore, it changed a bit during the course of a given experiment (owing to changing mole fraction of inerts in the gas phase), an effect that raised questions about one of the major approximations used in that model.

For the present, a new model for predicting the reaction kinetics from the transient pressure data was derived. The new model has only two unknown parameters and does not presume that the mass-transfer coefficient remains constant throughout the course of a given experiment (Rice et al., 1994). A clever way for providing agitation to the gas phase was introduced. This caused a large reduction in the gas-side resistance to mass transfer in the PRC, which made the process liquid-phase controlled, minimized the effects of gas-phase dilution, and, therefore, made all approximations in the model involving the gas phase less restrictive.

The heterogeneous cobalt catalyzed sulfite oxidation reaction

$$Na_2SO_3 + 1/2\,O_2 \xrightarrow{Co^{++}} Na_2SO_4,$$

was employed in this work. This reaction system was chosen because a number of investigations with different types of reactors have been performed to determine its kinetics under the conditions used in this work, and this provides a good basis for the comparison and validation of the current model. For example, Bub (1980a,b) and Wesselingh and Van't Hoog (1970) used both a wetted-wall column and a laminar jet, de Waal and Okeson (1966) used a wetted-wall column, and Alper and Abu-Sharkh (1988) used a stirred cell. Detailed considerations regarding the mechanism of the sulfite oxidation reaction are given by Bub (1980a) and Geary (1991).

Correspondence concerning this article should be addressed to R. G. Rice.
Current address of S. M. S. Soares: Engenho Novo Tecnologia Ltda., Rio de Janeiro/RJ, Brazil.

Pressure-Response Cell

The batch PRC employed in this investigation (Figures 1 and 2) is similar to that used in previous works, and a detailed description of the apparatus and method is given elsewhere (Rice et al., 1989). A fixed volume (750 mL) of liquid phase was in contact with a constant volume of gas, through a stable and flat gas-liquid interface of known area. The approximate placement of the interface is indicated in Figure 1. One component of the gas (oxygen) dissolved and reacted with the liquid-phase reactant (sodium sulfite), catalyzed by minute quantities of catalyst (cobalt sulfate). The PRC was constructed of Lexan, capped at each end and surrounded by a heat-exchanger jacket to insure isothermal operation. The experimental arrangement is illustrated in Figure 2.

The cell sat on top of a Drehzahl Electronics IKAMAG REO magnetic feedback controlled stirrer that provided direct readout of the stirring speed. A modified magnetic stir bar, capable of providing mixing to both the liquid and gas phases, was a major modification of this work. This modified stir bar consisted of a 1 1/8-in. (28.6-mm)-dia. by 1/2-in. (12.7-mm)-thick teflon cylinder which was machined to house

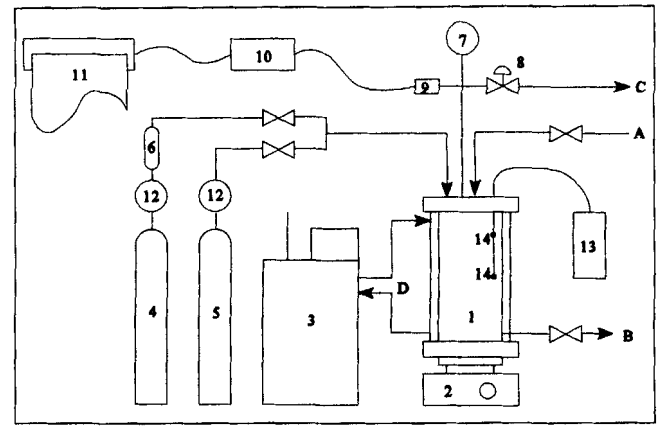

Figure 2. Pressure-response system.

(A) Inlet and vacuum port; (B) drain; (C) pressure relief; (D) cooling/heating-water recirculation; (1) pressure-response cell; (2) magnetic stirrer; (3) constant-temperature bath; (4) oxygen bottle; (5) nitrogen bottle; (6) water vapor saturator; (7) mechanical pressure gauge; (8) pressure relief valve; (9) pressure transducer; (10) digital pressure gauge; (11) strip chart recorder; (12) bottle pressure regulator; (13) temperature gauge; (14) temperature probes.

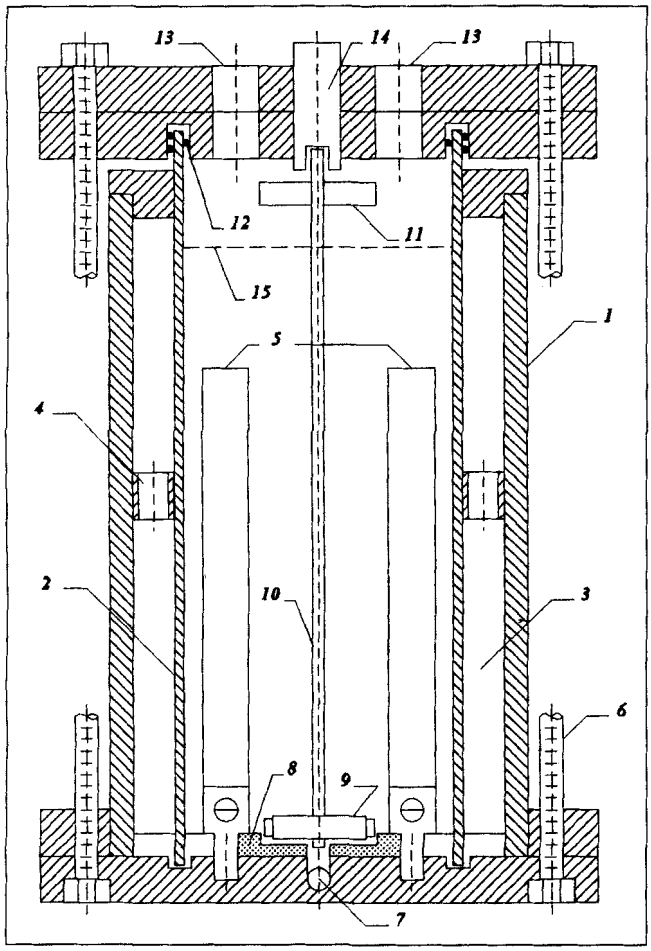

Figure 1. Pressure-response cell.

(1) Outer cylinder; (2) inner cylinder; (3) heat-exchanger jacket; (4) support rings; (5) baffles; (6) clamping bolts; (7) drain; (8) Teflon pad; (9) stir bar; (10) stir rod; (11) stir paddles; (12) o-ring seals; (13) inlet ports; (14) stir rod support; (15) gas-liquid interface.

a 1 1/2-in. (38.1-mm)-long by 3/8-in. (9.5-mm)-dia. magnetic stir bar. A 7 1/2-in. (190.5-mm)-long by 1/16-in. (1.6-mm)-dia. stainless steel rod was attached to the top of the teflon housing. Two 3/4-in. (19.1-mm)-long by 3/8-in. (9.5-mm)-wide rectangular plastic paddles were affixed 3/4 in. (19.1 mm) from the upper end of the rod, to provide the mixing to the gas phase. To avoid wobbling of the rod (which may induce waves and turbulence on the gas-liquid interface), its upper end was inserted into a Teflon bushing, as shown in Figure 1. The diameter of the hole was just slightly larger than that of the rod itself, so that it was able to turn freely.

The pressure-transient response was accomplished for the batch experiment via a pressure transducer placed through a piped-tee arranged on the top flange (Figure 2). The transducer was connected to a digital pressure gauge and a strip chart recorder, yielding pressure versus time data.

Transient Pressure Model

When the gas phase is mixed with inert diluent, such as nitrogen, the modeling of the transient pressure response is not straight forward. The concentration of the reacting gas dissolved in the liquid at the gas-liquid interface is no longer related to its partial pressure in the bulk of the gas phase by a simple linear relation, as used by Rice et al. (1994). Moreover, when a nonlinear reaction for the dissolved gas is taking place, the chemical liquid-phase mass-transfer coefficient, which is a function of the interfacial concentration of the reacting gas, becomes time-dependent, adding complexity to the problem.

If the reaction is taking place in the fast-reaction regime ($Ha > 3$), a mass balance contains an overall mass-transfer coefficient which includes gas film resistance and an effective liquid-phase mass-transfer coefficient for fast reactions in the liquid

$$\frac{V_G}{ART}\frac{dp_{A_G}}{dt} = -\frac{K_G}{RT}p_{A_G}, \qquad (1)$$

where p_{A_G} is the partial pressure of the reacting gas in the bulk of the gas phase, K_G is the overall gas-phase mass-transfer coefficient, and the concentration of dissolved gas (oxygen) in the bulk of the liquid is nil (fast reaction condition). The Hatta constraints were verified experimentally as illustrated in the Appendix. Mass-transfer coefficients were correlated as a function of power input into the liquid phase ($P = P_o\, \rho_L N^3 d_i^5$) (Soares, 1995), and yielded the following correlation: $Sh = 233 + 4.37 \times 10^{-5}\, Re^{1.5}$. The power number P_o is dimensionless and depends on geometry, baffle arrangement, and so on (Harnby et al., 1985; Holland and Chapman, 1966; Ulbrecht and Patterson, 1985).

Substituting the expression for the two-film resistance theory for chemical reaction

$$\frac{1}{K_G} = \frac{1}{k_G} + \frac{H}{RTk_R}, \tag{2}$$

into the mass balance equation yields

$$\frac{A}{V_G}dt = -\frac{1}{k_G}\frac{dp_{A_G}}{p_{A_G}} - \frac{H}{RTk_R}\frac{dp_{A_G}}{p_{A_G}}, \tag{3}$$

where the first term in the righthand side accounts for the gas-side resistance to mass transfer.

Rice and Beniot (1986) show that in the fast-reaction regime the effective liquid-phase mass-transfer coefficient is given by

$$k_R = \sqrt{\frac{2k_n D_{AL} C_A^{*n-1}}{n+1}}, \tag{4}$$

where C_A^* is the concentration of dissolved reactant gas in equilibrium with its partial pressure at the gas-liquid interface. Note, in the limit as $n \to 1$, $k_R = \sqrt{(k_1 D_{AL})}$.

The gas-phase mass-transfer coefficient, corrected for bulk transport when the diffusion is not equimolar, is given by

$$k_G = \frac{k_G^o}{(y_i)_{lm}}, \tag{5}$$

where $(y_i)_{lm}$ is the log-mean average of the mole fraction of inerts at the interface and bulk of the gas phase. When the flux of gas is small and the gas-side coefficient large, it is easy to see that the log-mean mole fraction of inerts for well mixed conditions does not differ appreciably from the mole fraction in the bulk of the gas phase, so that the following is a good approximation: $(y_i)_{lm} \approx y_{i_G}$ (Soares, 1995). Substituting this approximation into Eq. 5 and expanding the mole fraction in terms of the individual partial pressures of the gases

$$k_G = \frac{k_G^o}{y_{i_G}} = \frac{p_{i_G} + p_{A_G}}{p_{i_G}} k_G^o \tag{6}$$

Substituting Eqs. 4 and 6 into Eq. 3 yields

$$-\frac{A}{V_G}dt = \frac{1}{k_G^o}\frac{p_{i_G}}{p_{i_G} + p_{A_G}}\frac{dp_{A_G}}{p_{A_G}} + \frac{H}{RT}\left(\frac{n+1}{2k_n D_{AL} C_A^{*n-1}}\right)^{1/2}\frac{dp_{A_G}}{p_{A_G}}. \tag{7}$$

The first term on the righthand side accounts for the log-mean correction, and if k_G^o is large, its contribution is negligible. When the gas is not pure, C_A^* is the liquid-phase concentration of reacting gas in equilibrium with its partial pressure at the gas-liquid interface, and not in the bulk of that phase as would be the case for pure gas-phase systems (Rice and Benoit, 1986). However, when the gas-phase mass-transfer coefficient is very large, we may use the expression derived by Rice et al. (1994)

$$p_{A_G} = HC_A^* + \frac{RT}{k_G}\sqrt{\frac{2k_n D_{AL} C_A^{*n+1}}{n+1}} \approx HC_A^* \tag{8}$$

This considerably reduces the algebra for parameter estimation. If this approximation is used to replace C_A^* in Eq. 7 and the resulting equation is integrated between the limits $p_{AG}(0) = p_o$ and $p_{AG}(t) = p_{AG}$, the following pressure vs. time relation is obtained, even for nonlinear kinetics

$$t = \frac{V_G}{Ak_G^o}\ln\left[\frac{(p_{A_G} + p_{i_G})p_o}{(p_o + p_{i_o})p_{A_G}}\right] + \frac{2V_G}{(n-1)ART}\left[\frac{(n+1)H^{n+1}}{2k_n D_{AL} p_o^{n-1}}\right]^{1/2}\left[\left(\frac{p_{A_G}}{p_o}\right)^{(1-n)/2} - 1\right]. \tag{9}$$

It is easy to see that when $n = 1$ in Eq. 7, a simple exponential solution results (see Eq. 10, below). Typical for nonlinear systems, the dependent variable (p_{A_G}) is implicit. For any given experiment, it has only two unknown parameters, namely k_n, the pseudo-nth-order rate constant, and n the global reaction order with respect to the reacting gas. Therefore, a simple nonlinear parameter estimation routine can be used to determine the values of these two unknowns for any set of pressure vs. time data, provided k_G^o is found by independent means, as we discuss shortly.

Gas-Side Mass-Transfer Coefficient

As noted earlier, once a set of pressure (p_{A_G}) vs. time (t) data is collected for any given experimental run, Eq. 9 has only two unknown parameters n and k_n. All others are known either from the design of the PRC, the physical property data available in the literature, actual physical conditions, or from preliminary experiments. The values of A, interfacial area, and V_G, volume of the gas phase, were constant and taken from the calibration of the PRC (Soares, 1995): A was calculated from diameter measurements made with a caliper, and V_G was determined from pressure vs. volume data, as described by Bhargava (1988) and Soares (1995). The data for H was taken from Schumpe et al. (1978), and that for D_{AL} from the data of Bub (1980), Linek and Mayrhoferová (1970) and Reith and Beek (1973). The values of p_o, p_{i_G} and T were

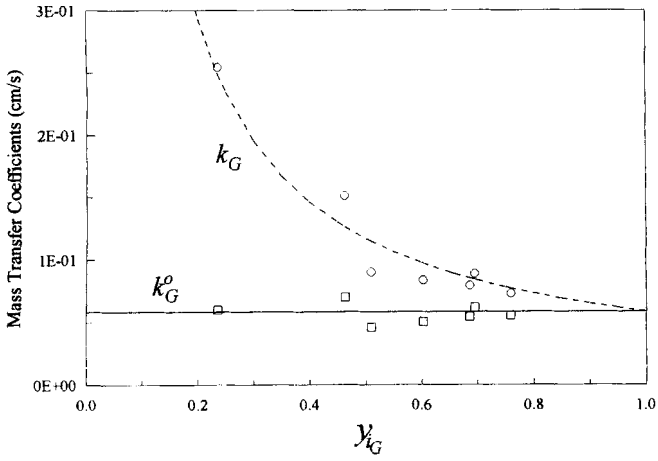

Figure 3. Gas-phase mass-transfer coefficients at 25°C and 1,100 rpm.

□ k_G^o; ○ k_G; solid line represents best fit of k_G^o; dashed line represents Eq. 6.

adjusted for each experiment, and monitored through the sensors indicated in Figure 2. Finally, the different k_G were calculated using the model derived by Rice et al. (1994), for reactions sustaining linear kinetics

$$p_{A_G} = p_o \exp\left[- \frac{\dfrac{At}{V_G}\sqrt{k_1 D_{AL}}}{\dfrac{H}{RT} + \dfrac{1}{k_G}\sqrt{k_1 D_{AL}}} \right], \qquad (10)$$

where k_1 is taken to be known using pure oxygen experiments ($k_G \to \infty$), as described by Rice and Benoit (1986). The sulfite oxidation reaction at high partial pressures of oxygen, $p_o > 1$ atm, was used in this procedure. A simple plot of $\ln(p_{A_G}/p_o)$ vs. time allows calculation of k_G. This is a function of y_{i_G} and stir speed, as shown in Figure 3.

At any given temperature and stir speed, the value of k_G was calculated for a number of different mole fractions of inert in the gas phase. The k_G vs. y_{i_G} data were then fitted into Eq. 6 to yield the value of k_G^o for that given temperature and stir speed. Figure 3 shows one such plot. Table 1 contains the values of the parameters present in Eq. 9. From the data for k_G^o, it is clear that the stirring of the gas phase was responsible for a considerable increase in its value, in comparison to those found by Rice et al. (1994), who used the same PRC without the mechanical gas mixing.

Determination of Kinetic Parameters and Parameter Estimation Routine

Equation 9 can be easily expanded to yield the global order of the gas-liquid reaction with respect to the liquid-phase reactant, catalyst, etc., as well as the activation energy for the chemical reaction. To determine the order of the reaction with the respect to a liquid-phase reactant or catalyst, the concentration of the desired species has to be made explicit as follows

$$k_n = k_{nm} C_B^m, \qquad (11)$$

Table 1. Physical Constants for the Heterogeneous Sulfite Oxidation Reaction

$A = 46.5$ cm^2 (measured, Soares, 1995)
$V_G = 125.0$ cm^3 (measured, Soares, 1995)
$D_{AL}(25°C) = 2.427\times10^{-5} - 1.351\times10^{-5}\, C_B + 1.146\times10^{-5}\, C_B^2 - 4.384\times10^{-6}\, C_B^3$ $D_{AL}(0.8\text{ M } SO_3^{=}) = 3\times10^{-6} + 8.25\times10^{-7}\, T - 1.125\times10^{-8}\, T^2 + 1.25\times10^{-10}\, T^3$, T, °C (Bub, 1980b; Linek and Mayrhoferová, 1970; Reith and Beek, 1973)
Solubility of Oxygen $H = 10^{0.346\, C_B} H^o$ where $H^o = 1.3924\times10^{79}\,(273.2+T)^{-24.45} \exp\left(-\dfrac{8748}{273.2+T}\right)$ T, °C (Schumpe et al., 1978)
$k_G^o = 4.57\times10^6 \exp(-5{,}461/T)$ T, K (Soares, 1995)

where k_{nm} is the (n, m)-order rate constant, C_B is the concentration of the species, and m is the reaction order with respect to that species. If a series of experiments is performed, so that all conditions are maintained the same, except for the concentration of the liquid-phase reactant (sodium sulfite) and the value of k_n determined independ-

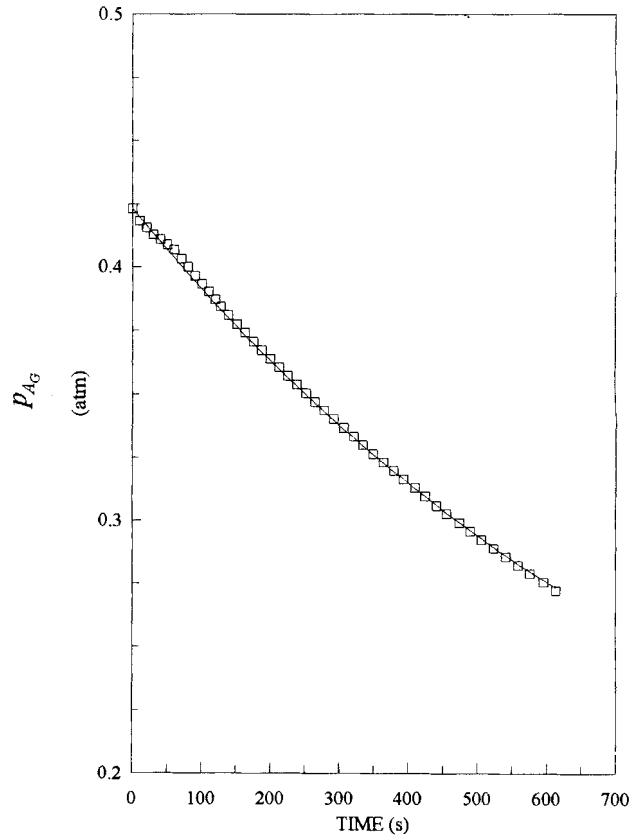

Figure 4. Partial pressure of oxygen (p_{AG}) vs. time.

0.5 M Na_2SO_3; 10^{-4} M Co^{+2}, pH 8.0; 25°C; 1,100 rpm; □ experimental data; solid line represents Eq. 9 with $n = 1.986$ and $k_n = 1.965\times10^9$.

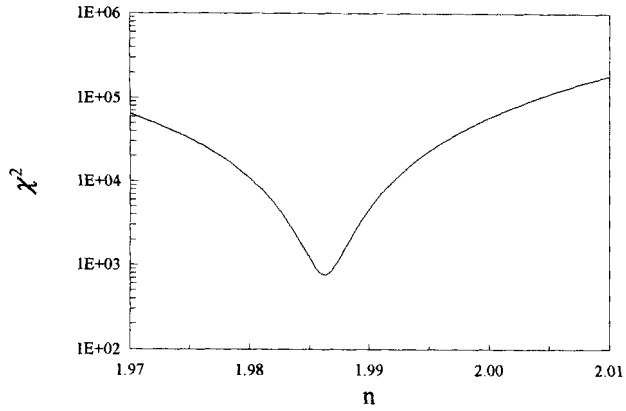

Figure 5. χ^2 around the optimal value of n ($n=1.986$); $k_n=1.965\times10^9$.

ently for each run, a plot of $\ln k_n$ vs. $\ln C_B$ gives a straight line with slope equal to m, the order in the liquid-phase reactant.

The procedure to determine the activation energy for the gas-liquid reaction is obtained via the Arrhenius relation. In this case, the pseudo-nth-order rate constant is expanded as

$$k_n = C\exp\left(-\frac{E_A}{RT}\right), \tag{12}$$

where E_A is the activation energy and C is the nth-order frequency factor. The activation energy is calculated from the values of k_n for a series of experiments performed at different temperatures. A plot of $\ln k_n$ vs. $1/T$ for these data yields a straight line of slope equal to $-E_A/R$, from which the activation energy is readily determined.

For use with the parameter estimation routine, Eq. 9 was first put in the following nondimensional form

$$\Phi = \ln\left[\frac{\Psi+\Theta}{(\Psi+1)\Theta}\right] + \frac{2k_G^o}{(n-1)RT}\left[\frac{(n+1)H^{n+1}}{2k_nD_Ap_o^{n-1}}\right]^{1/2}[\Theta^{(1-n)/2}-1], \tag{13}$$

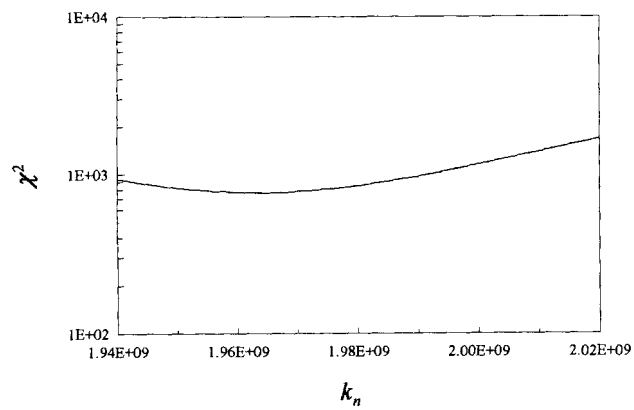

Figure 6. χ^2 around the optimal value of k_n ($k_n=1.965\times10^9$); $n=1.986$.

Table 2. Parameters Estimated for Low Pressure ($p_o<1$ atm) Sulfite Oxidation Reaction with Constant Stirring Speed (1,100 rpm)

T °C	p_{To} atm	p_o atm	Catalyst M	C_B M	n	k_n
25	2.04	0.41	1×10^{-4}	0.8	2.021	2.415×10^9
25	2.04	0.41	1×10^{-4}	0.8	2.019	1.983×10^9
25	4.83	0.83	1×10^{-4}	0.8	2.000	2.223×10^9
25	4.01	0.76	1×10^{-4}	0.8	1.984	2.237×10^9
25	3.47	0.76	1×10^{-4}	0.8	2.002	2.237×10^9
25	2.38	0.49	1×10^{-4}	0.8	1.946	2.107×10^9
25	2.04	0.42	1×10^{-4}	0.8	1.946	2.030×10^9
25	1.36	0.29	1×10^{-4}	0.8	1.951	2.131×10^9
25	2.04	0.42	1×10^{-4}	0.5	1.986	1.972×10^9
25	2.04	0.42	1×10^{-4}	0.6	1.943	1.945×10^9
25	2.04	0.41	1×10^{-4}	0.7	1.937	1.904×10^9
25	2.04	0.41	1×10^{-4}	1.0	1.939	2.022×10^9
25	2.04	0.41	5×10^{-5}	0.8	1.974	1.237×10^9
25	2.04	0.42	2×10^{-4}	0.8	2.005	4.335×10^9
25	2.04	0.42	5×10^{-4}	0.8	1.998	1.546×10^{10}
15	2.04	0.45	1×10^{-4}	0.8	1.960	1.457×10^9
38	2.04	0.42	1×10^{-4}	0.8	1.974	9.425×10^9
48	2.04	0.41	1×10^{-4}	0.8	1.968	1.510×10^{10}
18	2.04	0.42	1×10^{-4}	0.8	1.983	1.578×10^9
40	2.04	0.37	1×10^{-4}	0.8	1.981	8.820×10^9

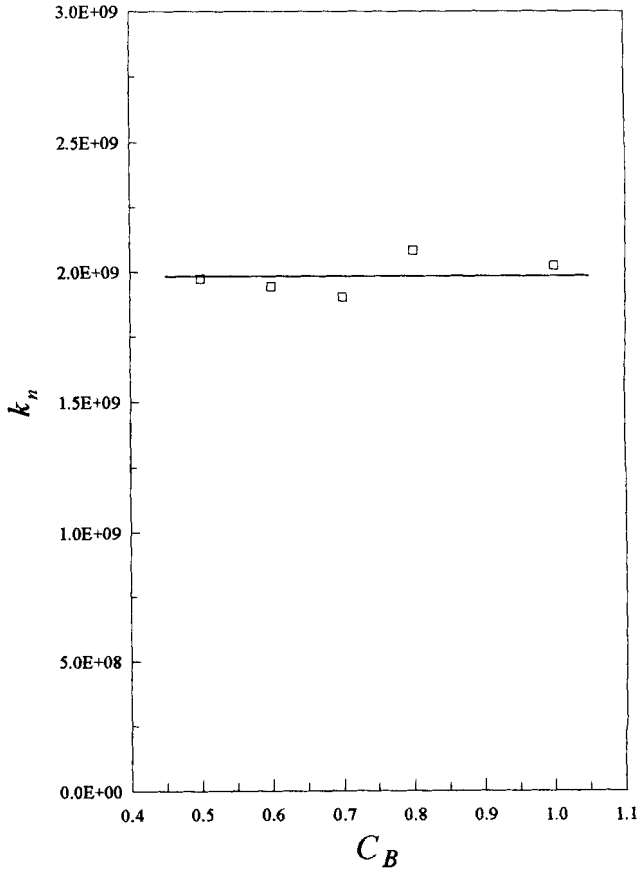

Figure 7. Pseudo-nth-order rate constant k_n vs. concentration of sulfite C_B (mol/L).

10^{-4} M Co^{+2}; pH 8.0; 25°C; 1,100 rpm; □ experimental data; solid line represents average value.

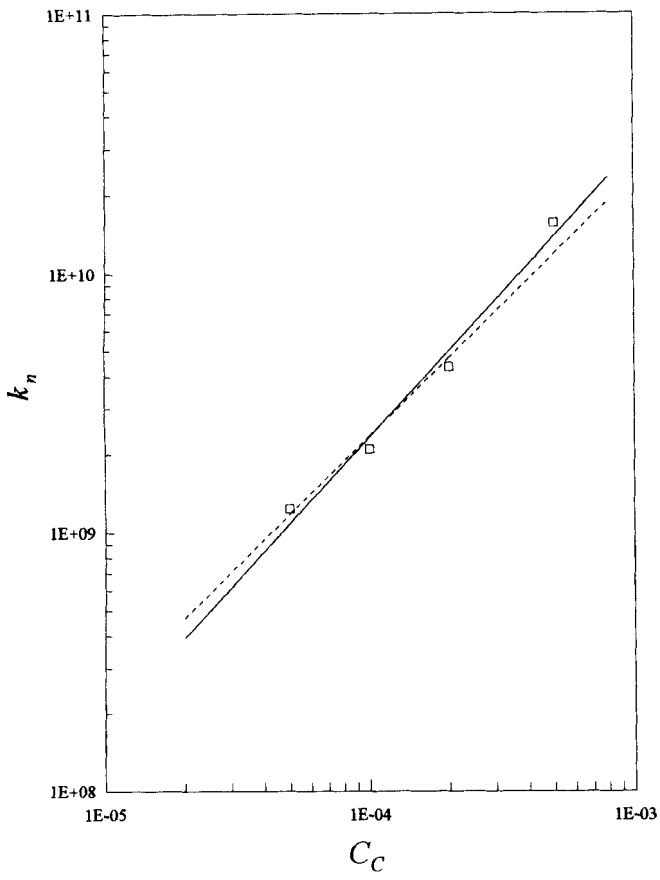

Figure 8. Pseudo-*n*th-order rate constant k_n vs. concentration of cobalt catalyst C_C (mol/L).

0.8 M Na_2SO_3; pH 8.0; 25°C; 1,100 rpm; □ experimental data; solid line represents fitted $m = 1.10$; dashed line represents $m = 1.0$.

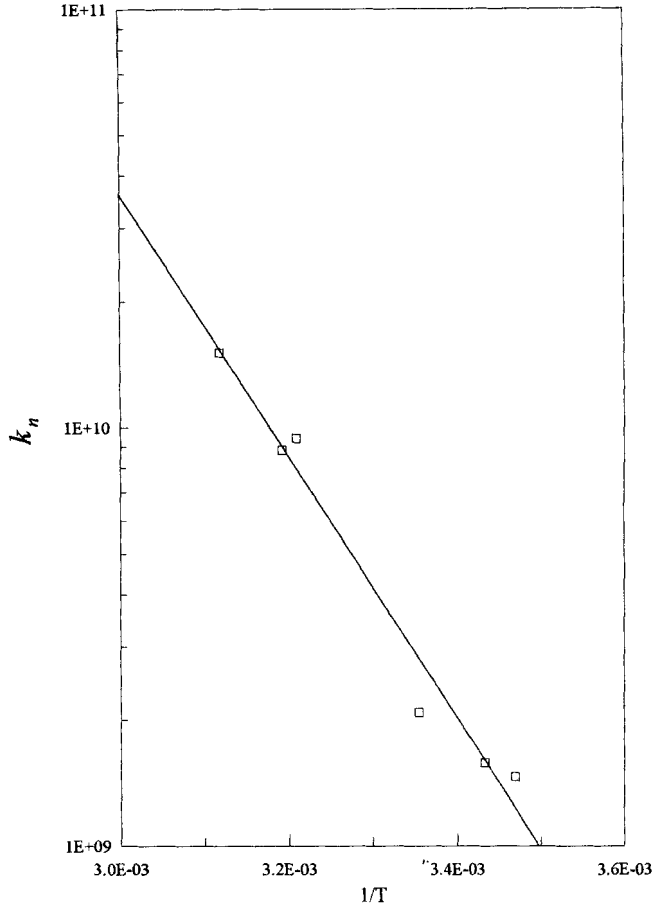

Figure 9. Pseudo-*n*th-order rate constant k_n vs. $1/T$.

0.8 M Na_2SO_3; 10^{-4} M Co^{+2}; pH 8.0; 1,100 rpm; □ experimental data; solid line represents fitted $E_A = 59.8$ kJ/mol.

where Φ is a dimensionless time, defined as $\Phi = Ak_G^o t/V_G$; Ψ is the dimensionless partial pressure of inert gas, defined as $\Psi = p_{i_G}/p_o$; and Θ is the dimensionless partial pressure of reacting gas, defined as $\Theta = p_{A_G}/p_o$. The two unknown parameters in Eq. 13 were determined with the aid of a quasi-Newton parameter estimation routine, the Levenberg-Marquardt method. The criterion function for all data fits was specified as the value of χ^2 between the experimental value of Φ and that obtained from Eq. 13. Figure 4 displays a sample best fit of the data. Figures 5 and 6 illustrate the values of χ^2 around the optimal values of n and k_n, respectively, for a given set of pressure vs. time data.

Assessment of the Kinetics of the Sulfite Oxidation Reaction ($p_o < 1$ atm)

The cobalt-catalyzed sulfite oxidation reaction, under the conditions where it is nonlinear with respect to the oxygen ($p_o < 1$ atm) (Bub, 1980a,b; Reith and Beek, 1973), was used to verify the predictions of the model. Experiments were performed at different conditions of initial partial pressure of oxygen, temperature, concentration of liquid-phase reactant, and concentration of catalyst. Table 2 shows the experimental conditions and the values predicted for n and k_n for several runs. The average value for n was 1.98 ± 0.02, which can be taken as $n = 2$. This is in excellent agreement with the literature, where an order of two for the oxygen is usually accepted for partial pressures below 1 atm (Bub, 1980b; Wesselingh and Van't Hoog, 1970), using a wetted-wall column and a laminar jet and using a wetted-wall column (Reith and Beek, 1973).

The model was also used to determine the order of the reaction in the sulfite ion. Figure 7 shows that the value of k_n did not change with the concentration of sulfite in solution. According to Eq. 11, this gives a zero-order dependence of the rate of reaction on the concentration of sulfite for concentrations above 0.5 M. This is exactly what is found in the literature (Bub, 1980b; de Waal and Okeson, 1966; Wesselingh and Van't Hoog, 1970).

In a similar manner, the order of the reaction in the cobalt catalyst was investigated. The slope of a plot of $\ln k_n$ vs. $\ln C_C$, where C_C is the concentration of catalyst, yielded an order of 1.1 ± 0.23 in C_C. Again, the agreement with the literature value of 1.0 (Alper and Abu-Sharkh, 1988; Reith and Beek, 1973; Wesselingh and Van't Hoog, 1970) is very satisfactory. In Figure 8, the experimental data, the calculated order of 1.1 and the literature order of 1.0 are plotted for reference.

Finally, the activation energy for the heterogeneous sulfite oxidation reaction was also calculated. Figure 9 contains the plot of $\ln k_n$ vs. $1/T$. The calculated activation energy was approximately 59.8 ± 5.3 kJ/mol (14.3 ± 1.3 kcal/mol). This

experimental parameter was in excellent agreement with the literature. Bub (1980b) reported exactly the same value, Reith and Beek (1973) found 58 kJ/mol, and Rice and Benoit (1986) found 58.1 kJ/mol for the first-order reaction in oxygen ($p_o > 1$ atm).

Conclusion

A simple modification to allow a magnetic stir bar to mix both liquid and gas phases caused a large increase in the value of the gas-phase mass-transfer coefficient. Consequently, the effect of diluting the gas had very little effect on the essential parameter estimation problem for PRC studies. The new model, with only two adjustable parameters, was capable of predicting the correct kinetics for the nonlinear heterogeneous cobalt catalyzed sulfite oxidation reaction, even in the presence of gas diluents, as compared to the results of other investigations using different types of reactors. This proved that the PRC is robust and sensitive enough to allow nonlinear kinetics to be estimated even under conditions of finite gas-phase resistance to mass transfer.

Notation

A = interfacial area, cm^2
C = nth-order frequency factor, units vary
C_A^* = equilibrium molar composition of reacting gas in the liquid phase, mol/L
C_B = concentration of liquid-phase reactant, mol/L
C_C = concentration of catalyst in the liquid phase, mol/L
d_i = liquid-phase impeller diameter, cm
D_{AL} = diffusivity of reacting gas in the liquid phase, cm^2/s
E_A = activation energy, kJ/mol
H = Henry's constant, $atm \cdot cm^3/mol$
Ha = Hatta number, k_R/k_L
k_1 = pseudo-1st-order rate constant, s^{-1}
k_G = gas-phase mass-transfer coefficient for diffusion through stagnant film, cm/s
k_G^o = gas-phase mass-transfer coefficient for equimolar counter-diffusion, cm/s
k_L = liquid-phase physical mass-transfer coefficient, cm/s
k_n = pseudo-nth-order rate constant, units vary
k_{nm} = (n, m)-order rate constant, units vary
k_R = liquid-phase mass-transfer coefficient with fast chemical reaction, cm/s
K_G = overall gas-phase mass-transfer coefficient, cm/s
m = order of the reaction in the liquid-phase reactant
N = stirring speed, rev./s
p_o = initial partial pressure of reacting gas, atm
p_{A_G} = partial pressure of reacting gas in the bulk of the gas phase, atm
p_{i_G} = partial pressure of inert gas in the bulk of the gas phase, atm
p_{T_O} = initial total pressure in the gas phase, atm
P = power input into the liquid phase, W
P_o = power number, dimensionless
q = stoichiometric coefficient of the chemical reaction (mol of B reacting with each mol of A)
R = universal gas constant, $atm \cdot cm^3/mol \cdot K$
Re = Reynolds number, Nd_i^2/ν
Sh = Sherwood number, $k_L d_i/D_{AL}$
t = time, s
T = temperature, K
V_G = volume of gas, cm^3
y_{i_G} = mole fraction of inert in the bulk of the gas phase

Greek letters

Θ = dimensionless partial pressure of reacting gas ($\Theta = p_{AG}/p_o$)
ν = kinematic viscosity of liquid, cm^2/s
ρ_L = liquid-phase density, g/cm^3

Literature Cited

Alper, E., and B. Abu-Sharkh, "Kinetics of Absorption of Oxygen into Aqueous Sodium Sulfite: Order in Oxygen," *AIChE J.*, **34**(8), 1384 (1988).

Astarita, G., *Mass Transfer with Chemical Reaction*, Elsevier, New York (1967).

Bhargava, S. P., "Pressure Response Cell: Determination of Non-Linear Kinetics," MS Thesis, Louisiana State Unv., Baton Rouge (1988).

Bub, G., "Cobalt-Catalyzed Autoxidation of Concentrated Aqueous Sodium Sulphite Solution I," *Oxidation Commun.*, **1**(3), 217 (1980a).

Bub, G., "Cobalt-Catalyzed Autoxidation of Concentrated Aqueous Sodium Sulphite Solution II," *Oxidation Commun.*, **1**(3), 233 (1980b).

de Waal, K. J. A., and J. C. Okeson, "The Oxidation of Aqueous Sodium Sulphite Solutions," *Chem. Eng. Sci.*, **21**, 559 (1966).

Geary, N. W., "On Bubble Columns," PhD Diss., Louisiana State Univ. (1991).

Harnby, N., M. F. Edwards, and A. W. Nienow, *Mixing in the Process Industries*, Butterworths, London (1985).

Holland, F. A., and F. S. Chapman, *Liquid Mixing and Processing in Stirred Tanks*, Reinhold, New York (1966).

Linek, V., and J. Mayrhoferová, "The Kinetics of Oxidation of Aqueous Sodium Sulphite Solution," *Chem. Eng. Sci.*, **25**, 787 (1970).

Reith, T., and W. J. Beek, "The Oxidation of Aqueous Sodium Sulphite Solutions," *Chem. Eng. Sci.*, **28**, 1331 (1973).

Rice, R. G., and E. L. Benoit, "An Experimental Pressure-Response Method to Measure Gas-Liquid Kinetics," *Chem. Eng. Sci.*, **41**(10), 2629 (1986).

Rice, R. G., J. A. King, and X. Y. Wang, "Absorption Kinetics and Mixing Studies in Pressure Response Cells," *Ind. Eng. Chem. Res.*, **28**, 1431 (1989).

Rice, R. G., L. F. Burns, and R. S. Miao, "Effect of Gas Diluents on Assessment of Kinetics in Pressure Response Cells," *Chem. Eng. Sci.*, **49**(6), 845 (1994).

Schumpe, A., I. Adler, and W. D. Deckwer, "Solubility of Oxygen in Electrolyte Solutions," *Biotechnol. Bioeng.*, **20**(1), 145 (1978).

Soares, S. M. S., "Parameter Estimation for Reactions of Nonlinear Kinetics in Pressure-Response Cells with Diluted Gas Phase," MS Thesis, Louisiana State Univ. (1995).

Ulbrecht, J. J., and G. K. Paterson, *Mixing of Liquids by Mechanical Agitation*, Gordon and Breach, New York (1985).

Wesselingh, J. A., and A. C. Van't Hoog, "Oxidation of Aqueous Sulphite Solutions: a Model Reaction for Measurements in Gas-Liquid Dispersions," *Trans. Instn. Chem. Engrs.*, **48**, T69 (1970).

Appendix

A number of experiments were performed to verify if the experimental data met the two Hatta constraints for the existence of the fast reaction regime (Astarita, 1967)

$$3 < Ha = \frac{k_R}{k_L} = \sqrt{\frac{2\,k_n D_{AL} C_A^{*n-1}}{(n+1)k_L^2}} \ll \frac{C_B}{q C_A^*} \qquad (14)$$

The physical mass-transfer coefficient was determined for the absorption of oxygen into 0.8 M solutions of sodium sulfate at various conditions of stir speed and temperature. The effect of stir speed on a physical mass-transfer coefficient is illustrated in Figure A1, and that of temperature in Figure A2. The second Hatta constraint was about 180. The Hatta number for the individual experiments varied between 40 for high speeds, and 75 for low speeds. Clearly both Hatta constraints are satisfied, and the reaction is in the fast reaction regime.

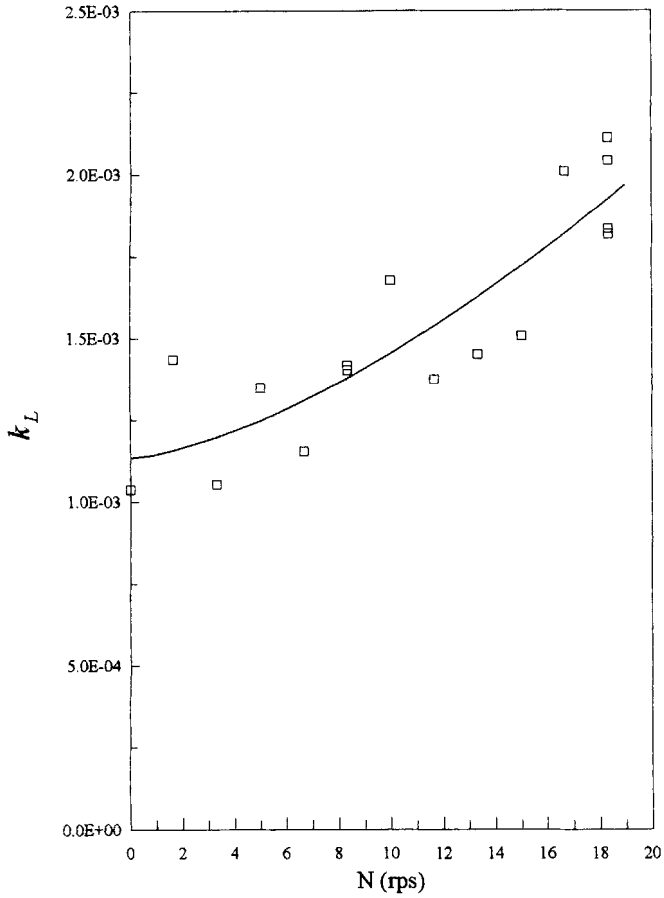

Figure A1. Physical mass-transfer coefficient k_L vs. stirring speed N.

0.8 M Na_2SO_4; pH 8.0; 25°C; □ experimental data; solid line represents fitted data.

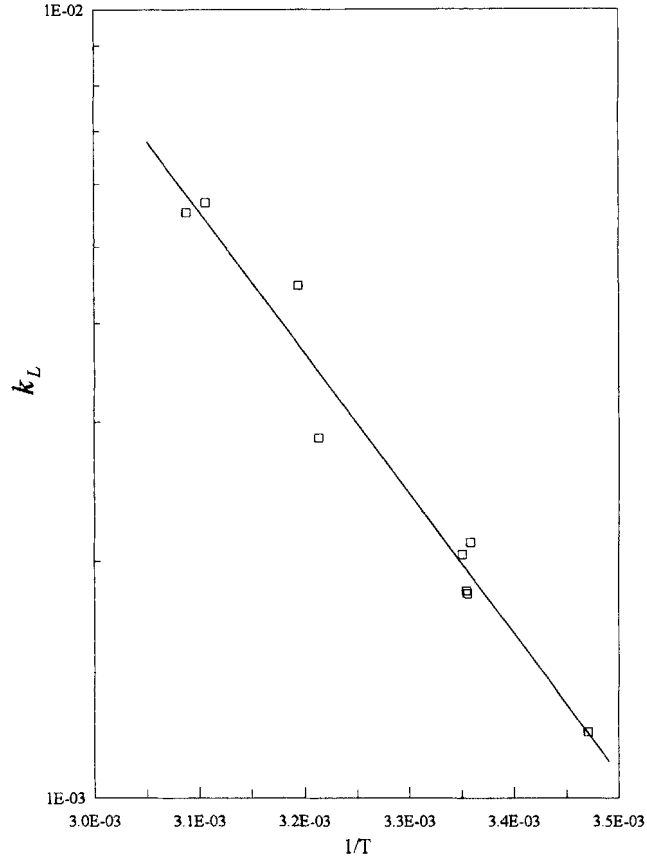

Figure A2. Physical mass-transfer coefficient k_L vs. $1/T$.

0.8 M Na_2SO_4; pH 8.0; 1,100 rpm; □ experimental data; solid line represents fitted data.

We can also check the approximation used in Eq. 8 where we show below as a sample calculation, that

$$HC_A^*(p_o) \gg \frac{RT}{k_G}\sqrt{\frac{2k_n D_{AL} C_A^{*n+1}}{n+1}} \qquad (15)$$

Sample calculation

Given: $T = 25$°C; $p_o = 0.8$ atm; $C_B = 0.08$ M Na_2SO_3; $C_C = 10^{-4}$M Co^{++}; $N = 18.3$ rps; $y_{i_G} = 0.8$; H, D_{AL} and k_G^o are taken from Table 1; and $n = 2$ and $k_n = 2\times10^9$ cm^3/mol·s. The lefthand side equals 0.8, and the righthand side approximately 0.02, which validates the approximation.

Manuscript received June 7, 1995, and revision received Sept. 18, 1995.